Semiannual Technical Report

Atomic Layer Epitaxy of Group IV Materials: Surface Processes, Thin Films, Devices and Their Characterization

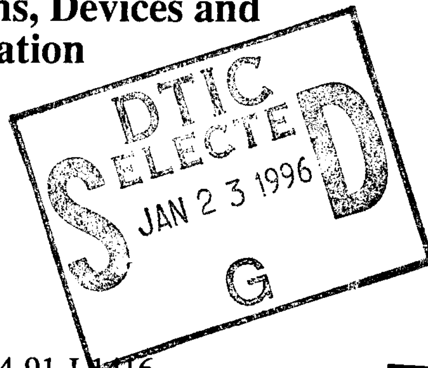

Supported under Grant #N00014-91-J-1416
Office of the Chief of Naval Research
Report for the period 7/1/95–12/31/95

19960117 038

R. F. Davis, S. Bedair*, N. A. El-Masry, Z. Sitar,
A. H. Morshed*, W. Liu, C. Wolden and P. Yang
c/o Materials Science and Engineering Department
and *Electrical and Computer Engineering Department
North Carolina State University
Campus Box 7907
Raleigh, NC 27695-7907

December, 1995

DTIC QUALITY INSPECTED 1

DISTRIBUTION STATEMENT A
Approved for public release;
Distribution Unlimited

REPORT DOCUMENTATION PAGE

Form Approved
OMB No. 0704-0188

Public reporting burden for this collection of information is estimated to average 1 hour per response, including the time for reviewing instructions, searching existing data sources, gathering and maintaining the data needed, and completing and reviewing the collection of information. Send comments regarding this burden estimate or any other aspect of this collection of information, including suggestions for reducing this burden to Washington Headquarters Services, Directorate for Information Operations and Reports, 1215 Jefferson Davis Highway, Suite 1204, Arlington, VA 22202-4302, and to the Office of Management and Budget Paperwork Reduction Project (0704-0188), Washington, DC 20503.

1. AGENCY USE ONLY *(Leave blank)*	2. REPORT DATE	3. REPORT TYPE AND DATES COVERED
	December, 1995	Semiannual Technical 7/1/95–12/31/95

4. TITLE AND SUBTITLE
Atomic Layer Epitaxy of Group IV Materials: Surface Processes, Thin Films, Devices and Their Characterization

5. FUNDING NUMBERS
414v001---01
1114SS
N00179
N66005
4B855

6. AUTHOR(S)
Robert F. Davis

7. PERFORMING ORGANIZATION NAME(S) AND ADDRESS(ES)
North Carolina State University
Hillsborough Street
Raleigh, NC 27695

8. PERFORMING ORGANIZATION REPORT NUMBER
N00014-91-J-1416

9. SPONSORING/MONITORING AGENCY NAMES(S) AND ADDRESS(ES)
Sponsoring: ONR, Code 312, 800 N. Quincy, Arlington, VA 22217-5660
Monitoring: Administrative Contracting Officer, ONR, Regional Office Atlanta
101 Marietta Tower, Suite 2805
101 Marietta Street
Atlanta, GA 30323-0008

10. SPONSORING/MONITORING AGENCY REPORT NUMBER

11. SUPPLEMENTARY NOTES

12a. DISTRIBUTION/AVAILABILITY STATEMENT
Approved for Public Release; Distribution Unlimited

12b. DISTRIBUTION CODE

13. ABSTRACT ***(Maximum 200 words)***
A seeding and multi-step deposition process has been developed to nucleate and grow oriented diamond films on both (100) and (111) Ni substrates without graphite codeposition, as shown by SEM and micro-Raman spectroscopy. Cross-sectional TEM and XRD confirmed the presence of a polycrystalline Ni_4C interlayer between single crystal Ni and the oriented diamond crystals. The key to the process is a molten Ni-C-H surface layer that promotes the nucleation of oriented particles and suppresses graphitic deposition. The presence of atomic hydrogen is critical to lowering the melting temperature of this surface layer. Based on the results of this work, a model is proposed to explain the mechanism of oriented diamond nucleation. In related work, diamond has been grown from a Ni-C solution in the presence of atomic hydrogen. Current work is focused on determining the nature of the surface molten phase, and attempts to grow heteroepitaxial diamond from the liquid phase. Atomic layer epitaxy of CeO_2 films on slightly off-oriented Si(100) substrates by pulsed laser ablation of a CeO_2 target was achieved under ultra high vacuum conditions and at low temperatures. RHEED patterns observed after RTA at 1000°C in Ar for 5 and 10 min indicated that crystallization was partially obtained. The effects of annealing in forming gas at 500°C for 30 min and subsequent RTA in Ar at 100°C for 5 min on the structure were investigated. The C-V and I-V properties of the films were investigated. The films have large MOS capacitance but also have larger leakage currents compared to those of epitaxial CeO_2 films on Si(111) substrates. However, improved leakage and breakdown characteristics were obtained with annealing in forming gas.

14. SUBJECT TERMS
diamond, nucleation, oriented films, Ni substrates, SEM, TEM, XRD, Ni_4C, atomic hydrogen, CeO_2, annealing, RTA, rapid thermal annealing, MOS capacitance, leakage currents, breakdown

15. NUMBER OF PAGES
26

16. PRICE CODE

17. SECURITY CLASSIFICATION OF REPORT	18. SECURITY CLASSIFICATION OF THIS PAGE	19. SECURITY CLASSIFICATION OF ABSTRACT	20. LIMITATION OF ABSTRACT
UNCLAS	UNCLAS	UNCLAS	SAR

NSN 7540-01-280-5500

Standard Form 298 (Rev. 2-89)
Prescribed by ANSI Std Z39-18
298-102

Table of Contents

I. Introduction 1

II. Nucleation and Growth of Oriented Diamond Films in the Ni-C-H System 3
C. Wolden, W. Liu, P. Yang, Z. Sitar and R. F. Davis

III. Properties of CeO_2 Films on Si(100) Substrates 21
A. H. Morshed, S. Bedair and N. A. El-Masry

IV. Distribution List 26

Accesion For		
NTIS CRA&I	☒	
DTIC TAB	☐	
Unannounced	☐	
Justification		
By		
Distribution /		
Availability Codes		
Dist	Avail and / or Special	
A-1		

I. Introduction

Atomic layer epitaxy (ALE) is the sequential chemisorption of one or more elemental species or complexes within a time period or chemical environment in which only one monolayer of each species is chemisorbed on the surface of the growing film in each period of the sequence. The excess of a given reactant which is in the gas phase or only physisorbed is purged from the substrate surface region before this surface is exposed to a subsequent reactant. This latter reactant chemisorbs and undergoes reaction with the first reactant on the substrate surface resulting in the formation of a solid film. There are essentially two types of ALE which, for convenience, shall be called Type I and Type II.

In its early development in Finland, the Type I growth scenario frequently involved the deposition of more than one monolayer of the given species. However, at that time, ALE was considered possible only in those materials wherein the bond energies between like metal species and like nonmetal species were each less than that of the metal-nonmetal combination. Thus, even if multiple monolayers of a given element were produced, the material in excess of one monolayer could be sublimed by increasing the temperature and/or waiting for a sufficient period of time under vacuum. Under these chemical constraints, materials such as GaAs were initially thought to be improbable since the Ga-Ga bond strength exceeds that of the GaAs bond strength. However, the self-limiting layer-by-layer deposition of this material proved to be an early example of Type II ALE wherein the trimethylgallium (TMG) chemisorbed to the growing surface and effectively prevented additional adsorption of the incoming metalorganic molecules. The introduction of As, however caused an exchange with the chemisorbed TMG such that a gaseous side product was removed from the growing surface. Two alternating molecular species are also frequently used such that chemisorption of each species occurs sequentially and is accompanied by extraction, abstraction and exchange reactions to produce self-limiting layer-by-layer growth of an element, solid solution or a compound.

The Type II approach has been used primarily for growth of II–VI compounds [1–13]; however, recent studies have shown that it is also applicable for oxides [14–17], nitrides [18], III–V GaAs-based semiconductors [19–32] and silicon [33–35]. The advantages of ALE include monolayer thickness control, growth of abrupt interfaces, growth of uniform and graded solid solutions with controlled composition, reduction in macroscopic defects and uniform coverage over large areas. A commercial application which makes use of the last attribute is large area electroluminescent displays produced from II–VI materials. Two comprehensive reviews [36,6], one limited overview [37] and a book [38] devoted entirely to the subject of ALE have recently been published.

In this reporting period, investigations concerned with (1) the implementation and development of a seeding and multi-step deposition process to nucleate and grow oriented

diamond films on both (100) and (111) Ni substrates without graphite codeposition and (2) the deposition and annealing of CeO_2 epitaxial films on Si(100) have been conducted.

The following sections introduce each topic, detail the experimental approaches, report the results to date and provide a discussion and a conclusion for each material. Each major section is self-contained with its own figures, tables and references.

References

1. T. Suntola and J. Antson, U.S. Patent 4,058,430, 1977.
2. M. Ahonen, M. Pessa and T. Suntola, Thin Solid Films **65**, 301, 1980.
3. M. Pessa, R. Makela, and T. Suntola, Appl. Phys. Lett. **38**, 131, 1981.
4. T. Yao and T. Takeda, Appl. Phys. Lett. **48**, 160, 1986.
5. T. Yao, T. Takeda, and T. Watanuki, Appl. Phys. Lett. **48**, 1615, 1986.
6. T. Yao, Jpn. J. Appl. Phys. **25**, L544, 1986.
7. T. Yao and T. Takeda, J. Cryst. Growth **81**, 43, 1987.
8. M. Pessa, P. Huttunen and M. A. Herman, J. Appl. Phys. **54**, 6047, 1983.
9. C. H. L. Goodman and M. V. Pessa, J. Appl. Phys. **60**, R65, 1986.
10. M. A. Herman, M. Valli and M. Pessa, J. Cryst. Growth **73**, 403, 1985.
11. V. P. Tanninen, M. Oikkonen and T. Tuomi, Phys. Status Solidi **A67**, 573, 1981.
12. V. P. Tanninen, M. Oikkonen and T. Tuomi, Thin Solid Films **90**, 283, 1983.
13. D. Theis, H. Oppolzer, G. Etchinghaus and S. Schild, J. Cryst. Growth **63**, 47, 1983.
14. S. Lin, J. Electrochm. Soc. **122**, 1405, 1975.
15. H. Antson, M. Leskela, L. Niinisto, E. Nykanen and M. Tammenmaa, Kem.-Kemi **12**, 11, 1985.
16. R. Tornqvist, Ref. 57 in the bibliography of Chapt. 1 of Ref. 38 of this report.
17. M. Ylilammi, M. Sc. Thesis, Helsinki Univ. of Technology, Espoo, 1979.
18. I. Suni, Ref. 66 in the bibliography of Chapt. 1 of Ref. 38 in this report.
19. S. M. Bedair, M. A. Tischler, T. Katsuyama and N. A. El-Masry, Appl. Phys. Lett. **47**, 51, 1985.
20. M. A. Tischler and S. M. Bedair **48**, 1681, 1986.
21. M. A. Tischler and S. M. Bedair, J. Cryst. Growth **77**, 89, 1986.
22. M. A. Tischler, N. G. Anderson and S. M. Bedair, Appl. Phys. Lett. **49**, 1199, 1986.
23. M. A. Tischler, N. G. Anderson, R. M. Kolbas and S. M. Bedair, Appl. Phys. Lett. **50**, 1266, 1987.
24. B. T. McDermott, N. A. El-Masry, M. A. Tischler and S. M. Bedair, Appl. Phys. Lett. **51**, 1830, 1987.
25. M. A. Tischler, N. G. Anderson, R. M. Kolbas and S. M. Bedair, SPIE Growth Comp. Semicond. **796**, 170, 1987.
26. S. M. Bedair in Compound Semiconductor Growth Processing and Devices for the 1990's, Gainesville, FL, 137, 1987.
27. J. Nishizawa, H. Abe and T. Kurabayashi, J. Electrochem. Soc. **132**, 1197, 1985.
28. M. Nishizawa, T. Kurabayashi, H. Abe, N. Sakurai, J. Electrochm. Soc. **134**, 945, 1987.
29. P. D. Dapkus in Ref. 27, in the bibliography of Chapt. 1 of Ref. 38 in this report.
30. S. P. Denbaars, C. A. Beyler, A. Hariz, P. D. Dapkus, Appl. Phys. Lett. **51**, 1530, 1987.
31. M. Razeghi, Ph. Maurel, F. Omnes and J. Nagle, Appl. Phys. Lett. **51**, 2216, 1987.
32. M. Ozeki, K. Mochizuki, N. Ohtsuka, K. Kodama, J. Vac. Sci. Technol. **B5**, 1184, 1987.
33. Y. Suda, D. Lubben, T. Motooka and J. Greene, J. Vac. Sci. Technol. **B7**, 1171, 1989.
34. J. Nishizawa, K. Aoki, S. Suzuki and K. Kikuchi, J. Cryst. Growth **99**, 502, 1990.
35. T. Tanaka, T. Fukuda, Y. Nagasawa, S. Miyazaki and M. Hirose, Appl. Phys. Lett. **56**, 1445, 1990.
36. T. Suntola and J. Hyvarinen, Ann. Rev. Mater. Sci. **25**, 177, 1985.
37. M. Simpson and P. Smith, Chem. Brit. **23**, 37, 1987.
38. T. Suntola and M. Simpson, *Atomic Layer Epitaxy*, Chapman and Hall, New York, 1990.

II. Nucleation and Growth of Oriented Diamond Films in the Ni-C-H System

A. Introduction

The growth of highly oriented heteroepitaxial films represents an important step toward the attainment of large-area, device-quality diamond [1-3]. It has been known for decades that Ni and other transition metals are effective solvent-catalyst metals for diamond crystallization under high pressure and high temperature (HPHT) conditions [4]. The properties of diamond and the transition metals are shown in Table I. Nickel was chosen as a substrate material in this research because of its close lattice match (1.13%).

Table I. The Properties of Diamond and the Transition Metals

Mater.	Electron Configur.	Crystal Structure	Lattice Const. (20°C, Å)	Density (20°C, g/cm^3)	Melt. Point (°C)	Coeff. Thermal Expansion (20°C, 10^{-6}/°C)	Electrical Resistivity (20°C, μohm-cm)	Hydrogen Solubility (1 atm., ppm)	Me-C Eutectic M.P. (°C, wt.%C)	Carbides	Hydrides
Diam.	[He]$2p^2 2s^2$	fcc	3.56	3.52	3830	0.8	10^{14-16}	—	—	—	—
Ni	[Ar]$3d^8 4s^2$	fcc	3.52	8.91	1453	13.3	6.8	200 (420°C) 500 (900°C)	1326 (2.2%)	Ni_3C	NiH
Co	[Ar]$3d^7 4s^2$	hcp (α-Co) <417°C fcc (β-Co) >417°C	a=2.51 c=4.07 3.55	8.92	1495	12.5	6.2	65 (700°C) 134 (900°C)	1320 (2.6%)	Co_3C Co_2C	CoH CoH_2
Fe	[Ar]$3d^6 4s^2$	bcc (α-Fe) <912°C fcc (γ-Fe) >912°C	2.87 3.65	7.87	1536	12.6	9.7	120 (800°C) 250 (1000°C)	1147 (4.3%)	Fe_3C	x
Mn	[Ar]$3d^5 4s^2$	bcc(α-Mn) <727°C cub(β-Mn) >727°C	8.89 6.29	7.43	1245	22.8	185	600 (400°C) 1400 (800°C)	1231 (min. M.P. at 0.3%)	$Mn_{23}C_6$ Mn_3C Mn_5C_2 Mn_7C_3	MnH
Cr	[Ar]$3d^5 4s^1$	bcc	2.88	7.19	1875	6.2	12.9	13 (400°C) 44 (800°C)	1534 (3.6%)	$Cr_{23}C_6$ Cr_7C_3 Cr_3C_2	CrH CrH_2

The strong catalytic effect of Ni on hydrocarbon decomposition and subsequent graphite formation at low pressures have prevented CVD diamond nucleation on the Ni surface without the deposition of an intermediate graphite layer [5]. A graphite interlayer generally forms immediately when Ni substrates are placed in a methane-hydrogen CVD environment [6].

However, Badzian and Badzian [7] found that graphite formation is inhibited when Ni first forms a nickel hydride. In addition, Sato *et al.* and Fujita *et al.* [8] reported that both <111> and <100> oriented diamond nuclei could be grown on Ni substrates. However, the amount of orientation was rather limited, and no details were given about the deposition process.

Work that has led to the achievement of oriented diamond growth on Ni in the Ni-C-H system is reported here. We describe the process, characterize the deposited films, and develop a model to explain the nucleation mechanism. In addition, the results of diamond growth from the liquid phase are reported. Current investigations and plans for future work are reviewed.

B. Experimental

Oriented Diamond Growth. The experiments were carried out in both hot-filament and microwave CVD systems. Both (100) and (111) single crystal Ni and polycrystalline Ni were used as substrates. Substrates were polished using standard metal polishing techniques, the final polish being accomplished with a 1 μm diamond aerosol. Samples were then cleaned with trichloroethylene, acetone, and DI water. For subsequent seeding, the substrates were simply immersed in a diamond /acetone suspension, and a layer of diamond powders (<2 mm) was left on the Ni surfaces when the samples were removed.

The nucleation and growth was conducted through a three-step process including: deoxidation (step 1); high temperature annealing (step 2); and a standard diamond growth conditions (step 3) as shown in Fig. 1. Step 1 involved annealing the seeded substrates at a temperature of 900 °C in a hydrogen atmosphere for 10-30 minutes to remove oxides from the substrate surface.

In the hot filament CVD system, the substrates were heated by radiative heating from the tungsten filaments without an external heater. All cited temperatures were calibrated by the melting points of Ge and Ni-Cu alloys, as well as thermocouples attached to the substrate surface.

For step 2, the substrate temperature was raised to about 1100°C while the tungsten filament was held at a temperature of approximately 2300°C. At this high temperature and in the presence of atomic hydrogen the diamond seeds started to dissolve rapidly into the Ni lattice. The high temperature annealing time varied depending on the degree of seeding and the exact surface temperature. It is believed that the annealing time must be long enough to permit sufficient reaction between the nickel, diamond seeds, and hydrogen to form a Ni-C-H intermediate layer which suppresses graphite formation and promotes diamond nucleation. After the high temperature anneal, the substrate temperature was lowered to about 900°C and CH_4 gas flow at 0.5% was started to begin diamond growth. The experimental conditions of the multi-step process are summarized in Table II.

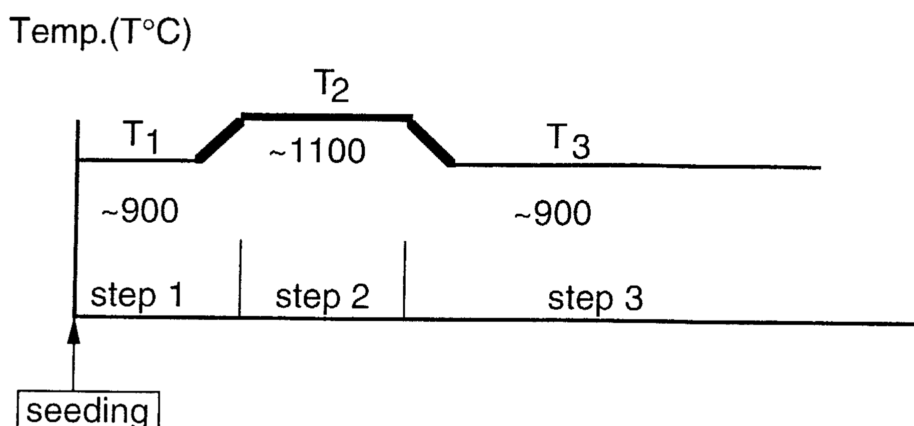

step1: de-oxidation
step2: high temperature annealing to form Ni-C-H surface phases
step3: nucleation and growth

Figure 1. The schematic diagram of the seeding and multi-step process.

Table II. Experimental Conditions of the Multi-step Process

	Substrate Temperature [°C]	CH_4/H_2 Flow Rate [sccm]	Duration Time
Step 1 Deoxidation	900	0/400	10-30 minutes
Step 2 High Temp Anneal	1100	0/400	10-60 minutes
Step 3 Regular Growth	900	2/400	4-20 hours

*P = 30 torr at all times

In practice, the duration of the anneal was effectively controlled by the visual appearance of the seeded substrates. The surface would change from dark gray in the initial annealing stage to reflective or "shiny" when the desirable Ni-C-H surface layer was formed. Laser reflection measurements were used to detect the surface reflectivity changes during the multi-step process. A HeNe laser beam was directed at the substrate and the reflection intensity was monitored. Figure 2 shows a typical intensity curve during the multi-step process. Initially the reflective light intensity is very low, because the light was scattered by the carbon seeds on the surface.

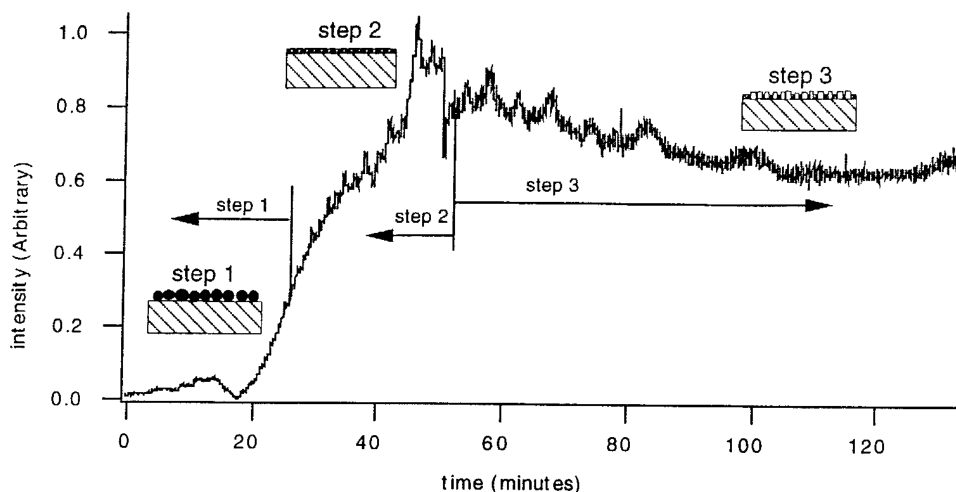

Figure 2. Laser reflection monitoring of the seeding and multi-step process.

The reflected light intensity increased rapidly when the substrate temperature was raised to about 1100°C where it approached a saturated value, possibly indicating the formation of a molten surface layer.

TEM Analysis of Oriented Growth Mechanism. To provide insight into the mechanism of diamond orientation on Ni plan-view and cross-section TEM samples of the oriented diamond on Ni were made. The plan-view samples were prepared by the standard method. For cross-section samples difficulties were encountered since diamond is hardest material known, and Ni is very soft. The following technique was developed to overcome some of the difficulties. Two samples are glued together with diamond particles sides face to face. Then the sample is placed into copper or molybdenum tube and cut into slices about 400 μm thick. The slice is first flatted, dimpled, and polished to 60 μm on one side. Then the sample is turned over and further ground and polished to the minimum thickness possible. Finally, the sample is ion milled by using "sector rotation speed control," which rotates the specimen slowly when the ion beam is perpendicular to the layer in the specimen and rapidly through the remaining sectors. Although time-consuming, this procedure was found to successfully yield TEM samples from which high quality micrographs were obtained.

Liquid Phase Diamond Growth. A liquid phase diamond growth method has been developed to grow diamond from a Ni-C solution in an atomic hydrogen environment at low pressures. The experiment was conducted in a HFCVD system, as shown in Fig. 3. Nickel and graphite (2.3 wt%) powders are mixed and put into an alumina crucible. As a reference, at 2.2 wt% nickel and carbon form a eutectic at 1327°C at atmospheric pressure. The crucible is then placed under a tungsten filament which is maintained at a temperature of 2300°C. The Ni and C powders are heated to a molten state and kept there for about 3 hours in a hydrogen ambient. The molten Ni-C solution is cooled down to room temperature. The resulting solid

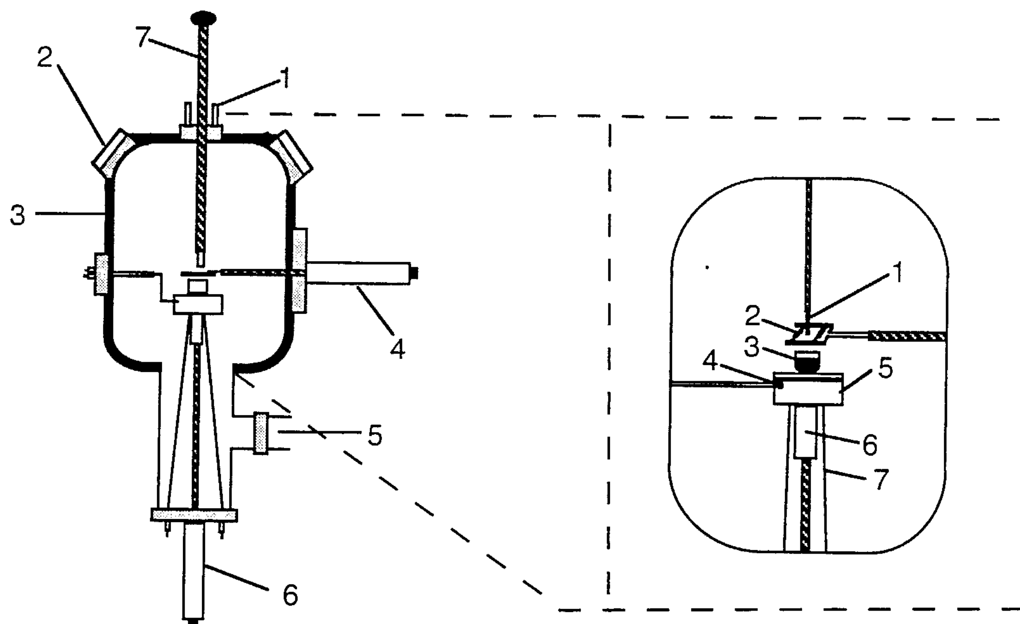

1--Gas Inlet
2--Viewports
3--Water Cooling
4--Linear Transfer for filament
5--to Pump
6--Sample Manipulator
7--Seed Holder

1--Seed
2--Filaments for creating atomic H
3--Crucible
4--Thermocouple for controlling growth temperature
5--h-BN heater
6--h-BN support
7--Heater wires

Figure 3. System for diamond growth.

assumes a ball-like shape due to surface tension. During the cool down process supersaturated carbon precipitates on the surface in the form of diamond particles.

C. Results

Oriented Diamond Growth. The oriented diamond films grown on Ni substrates using diamond seeding were first investigated by scanning electron microscopy (SEM). Figures 4 and 5 show SEM micrographs of oriented diamond films deposited by HFCVD on single-crystal (111) and (100) Ni, respectively. Micro-Raman was performed by focusing an argon laser, at a wavelength of 514.5 μm, on the diamond surface with a spot size of approximately 5 μm. A representative Raman spectrum is shown in Fig. 6, confirming the high-quality of the diamond. A very small amount of graphite (no amorphous sp^2C) is observed on the substrate areas not covered by the diamond nuclei.

X-ray diffraction has been utilized to probe the formation of an interfacial carbide phase [9]. A high nucleation density diamond film was prepared using the multi-step process on a single-crystal {100} Ni substrate. A micrograph of the high density film is presented in

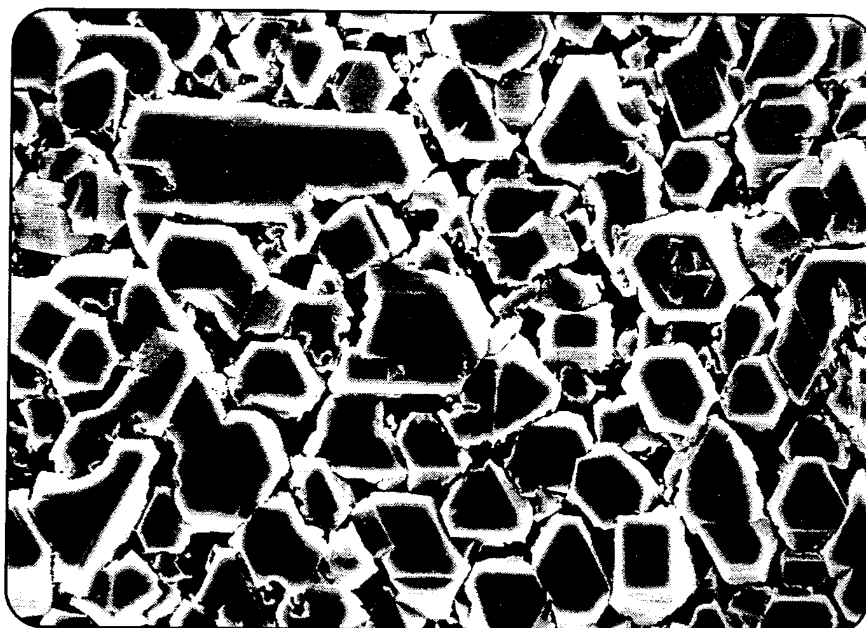

Figure 4. SEM micrographs of diamond films grown on a (111) oriented single crystal Ni surface. (a) An overview at low magnification and (b) a high magnification image.

Figure 5. The 45° tilted SEM micrograph of a (100) oriented diamond film on a Ni substrate.

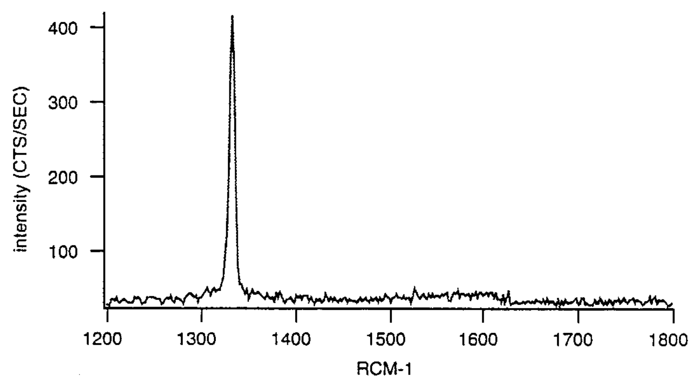

a

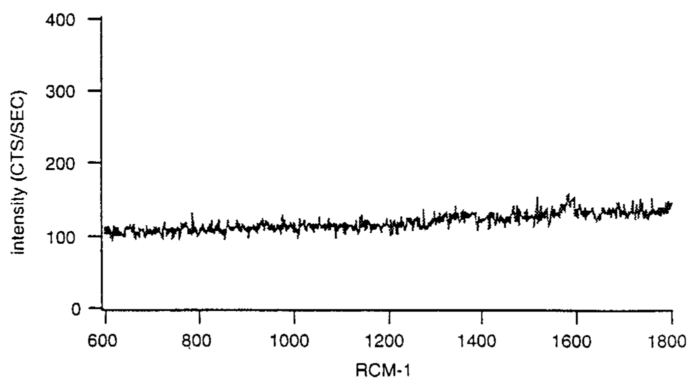

b

Figure 6. (a) A typical Raman spectrum from the diamond nuclei and (b) Raman spectrum from the substrate not covered by the diamond nuclei.

Fig. 7, which clearly shows coalescence of the (100) oriented diamond particles. Phase identification by X-ray diffraction (XRD) was undertaken using the wide-film Debye-Scherrer X-ray technique developed by Read. The XRD photograph from the diamond on nickel sample is shown in Fig. 8. Generally speaking, the observed diffraction pattern consists of two components: (i) a set of strong diffraction spots from the single crystal Ni substrate; and (ii) weaker diffraction lines from the thin film growth. The latter component may be further divided into lines of two types: (a) a set of "grainy" lines from a phase or phases exhibiting a large grain (°5 μm) structure; and, (b) a set of smooth lines from a phase or phases exhibiting a small grain structure (<5 μm). The XRD data is summarized in Table III.

Table III. X-ray Diffraction Data from a (100) Oriented Diamond Film on Ni

Actual Data	d (Å)	structure (hkl) [intensity in brackets]
5.19	3.593	
5.52	3.273	3.348 (002) [100] graphite
7.96 (S+G)	2.022	2.039 (111) [100] Ni_4C
same	same	2.027 (101) [15] graphite
same	same	2.06 (111) [100s] diamond
9.10 (S)	1.744	1.765 (200) [80] Ni_4C
13.34 (G)	1.259	1.261 (220) [25] diamond
13.64 (S)	1.243	1.259 (022) [60] Ni_4C

In particular, "grainy" lines are observed at d spacings of 2.03 Å and 1.26 Å which is attributable to diffraction from diamond crystallites [d=2.06 Å for the {111} diamond and d=1.26 Å for {220} diamond]. This interpretation is bolstered by SEM images that show identifiable diamond crystallites with grain sizes on the order of 5 μm (see Fig. 7). Furthermore, smooth lines are found in similar positions: 3.32; 2.03-04, 1.75 and 1,24 Å, essentially coincident with the "grain" diamond lines.

It appears that small graphite crystallites contribute to the lines at 3.32 Å [d=3.35 Å for {100} graphite] and 2.03-2.04 Å [d=2.03 Å for {101} graphite]. Small grains of cubic Ni_4C phase may be associated with the smooth lines at 2.03-2.04 Å [d=2.04 Å for {111} Ni_4C], 1.75 Å [d=1.75 Å for {200} Ni_4C], and 1.24 Å [d=1.26 Å for {022} Ni_4C].

The X-ray scattering results indicate the presence of three phases in the thin film deposition. Diffraction from diamond crystallites with relatively large grain sizes dominates, but weaker and smoother lines from graphite and Ni_4C crystallites with relatively small grain sizes are readily detected. The presence of the graphitic phase is not particularly surprising

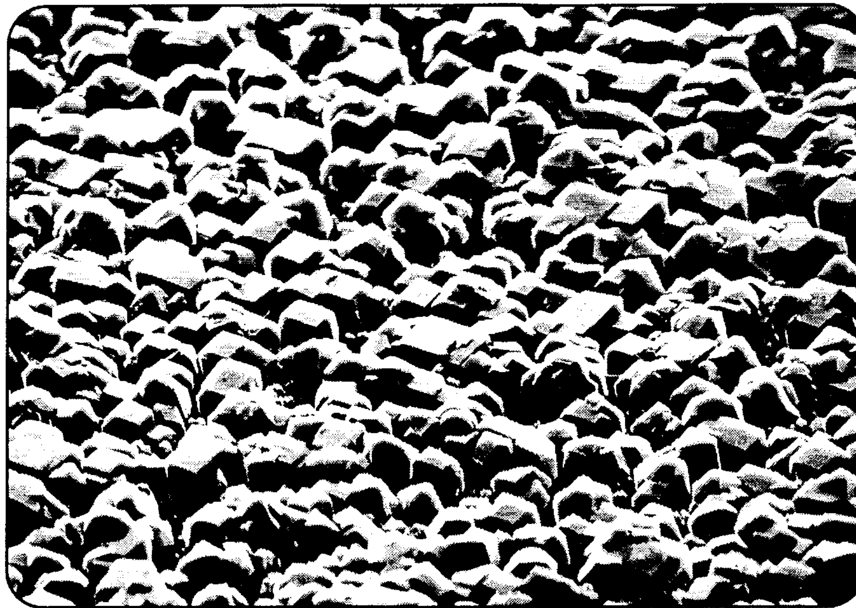

Figure 7. SEM micrograph of high density (100) oriented diamond film on a Ni substrate which is used in the x-ray diffraction analysis.

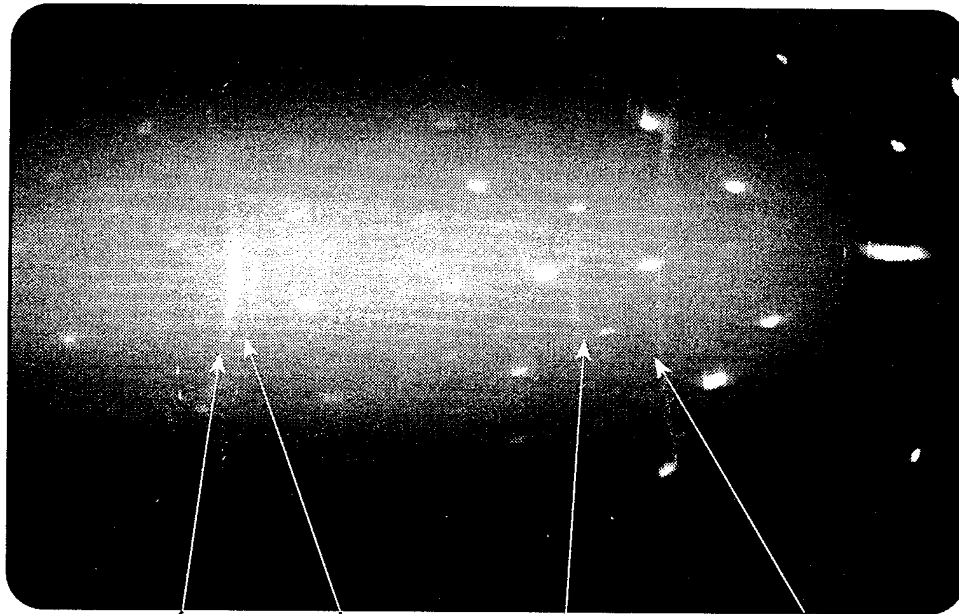

Figure 8. X-ray diffraction photograph of the high density (100) oriented diamond film on the (100) single crystal Ni substrate.

because the deposition conditions are not entirely uniform across the whole substrate. More importantly the X-ray diffraction lines are consistent with the presence of a metastable Ni_4C phase which is normally very difficult to detect due to the broad overlap of polycrystalline X-ray patterns for Ni, diamond, and Ni_4C. The observed separation of the scattering vectors from these three components is somewhat fortuitous, and is attributed to the single-crystal nature of the Ni substrate and the difference in the grain sizes of the diamond and Ni_4C phases.

It can be seen that the {022} and {200} Ni_4C lines are relatively strong compared to the {111} lines of diamond. This suggests that the C/Ni ratio is at least 25% [10,11]. The Ni_4C is in a NaCl structure with carbon atoms in the octahedral interstitial sites.

TEM Analysis of Oriented Growth Mechanism. A cross-section TEM specimen was prepared from a sample of oriented diamond on Ni after 4 hours of growth. Figure 9 shows a TEM micrograph of two oriented diamond particles which was attained after the sample preparation discussed above. There are three distinct regions in Fig. 9: (i) the diamond crystal, (ii) the Ni substrate, and (iii) an irregular interlayer of Ni_4C approximately 0.5 mm thick. SAD analysis (photographs also shown in Fig. 9) clearly identifies each phase.

The (200) ring is the special diffraction line which shows the presence of the Ni_4C phase. From the ring pattern, it can be concluded that the fine grain polycrystalline Ni_4C phase was formed between diamond and Ni substrate. For diamond the (200) reflection is forbidden,

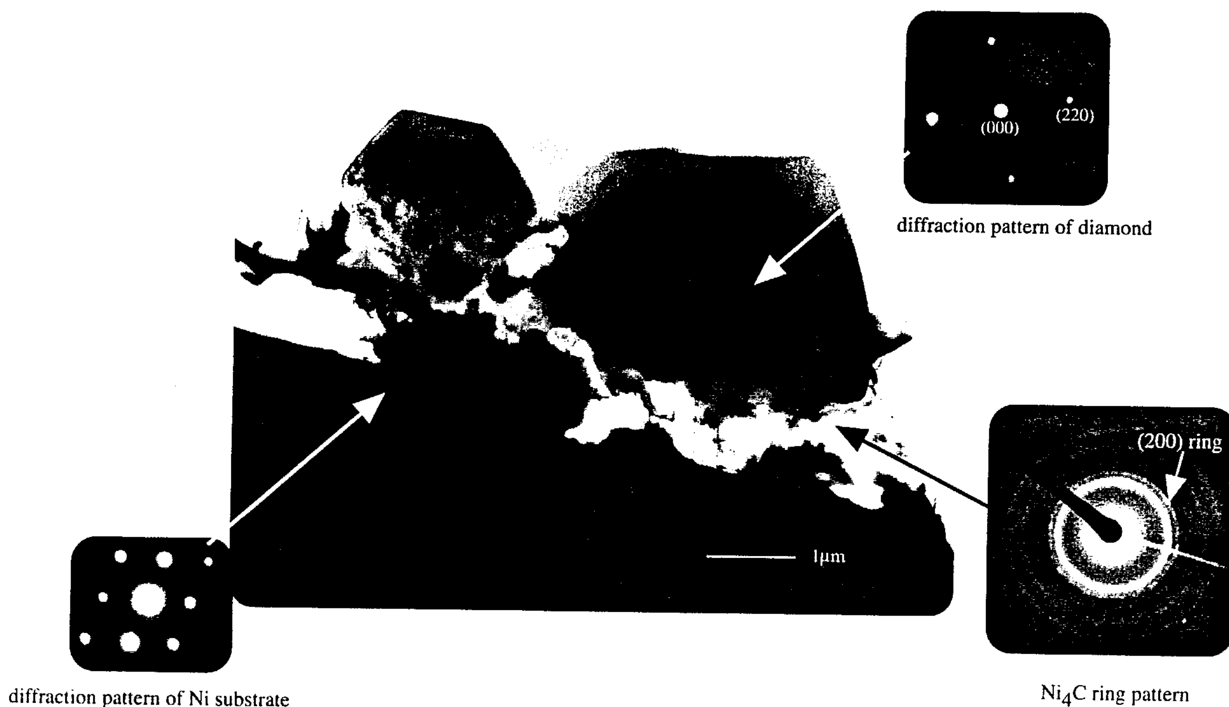

Figure 9. Cross-section TEM analysis of the interfacial Ni_4C phase involved in the nucleation and growth of oriented diamond on Ni.

although it may be allowed if the particles are either defective or too small. However, the SEM micrographs show relatively large (°5 mm) crystallites and there are no signs of twinning or other macroscale defects. The [100] zone axis diffraction pattern can be used to identify the diamond as shown in Fig. 9.

Liquid Phase Diamond Growth. Figure 10 shows the SEM micrographs of diamond particles grown on the surface of the molten Ni-C ball. Figure 11 shows the Micro-Raman spectrum obtained from these diamond particles. As only hydrogen gas was present, the results demonstrate that the carbon is supplied from the liquid phase, not the vapor phase. The melting point of the Ni-C solution is reduced appreciably by atomic H to about 1100°C. Also, it is speculated that the solubility of C in Ni may be enhanced by the presence of atomic hydrogen. The experimental results show that diamond can be grown from a liquid phase.

D. Discussion

Oriented Diamond Growth. Based on experimental evidence from the multi-step deposition process, the model shown schematically in Fig. 12, was proposed to understand the mechanism of oriented nucleation and growth of diamond on nickel substrates. In the first step a single crystal nickel substrate is seeded with carbon powders, either diamond or graphite. When the seeded substrate is heated to about 1100°C in a hydrogen atmosphere reactions among nickel, carbon, and atomic hydrogen occur and eventually lead to the formation of a molten, Ni-C-H eutectic compound on the surface. These two steps can also be accomplished by saturating the nickel surface with gaseous carbon species at 1100°C.

During the subsequent cooling to a substrate temperature of 900-950°C diamond nucleation is initiated from the molten eutectic compound at the surface, which is now anticipated to be supersaturated with carbon. The diamond nuclei grow with an epitaxial relationship to the substrate which has a very close lattice constant to that of diamond. Finally, diamond grows out from the nuclei and forms oriented diamond particles using normal CVD diamond growth conditions.

This model emphasizes the importance of forming a molten Ni-C-H surface layer during the high temperature anneal in hydrogen. Evidence for this can be seen in the area surrounding oriented diamond particles on nickel, where flow patterns have been observed on the substrate using contrast microscopy, as shown in Fig. 13. The step increase in the reflection intensity shown in Fig. 2 is also consistent with surface melting.

For the observed surface melting to occur at 1100°C or below, atomic hydrogen must play an important role in the depression of the eutectic melting point. Badzian has also reported the melting of Ni at 1150°C when annealed in a hydrogen plasma [7], much below the melting point of Ni at 1450°C.

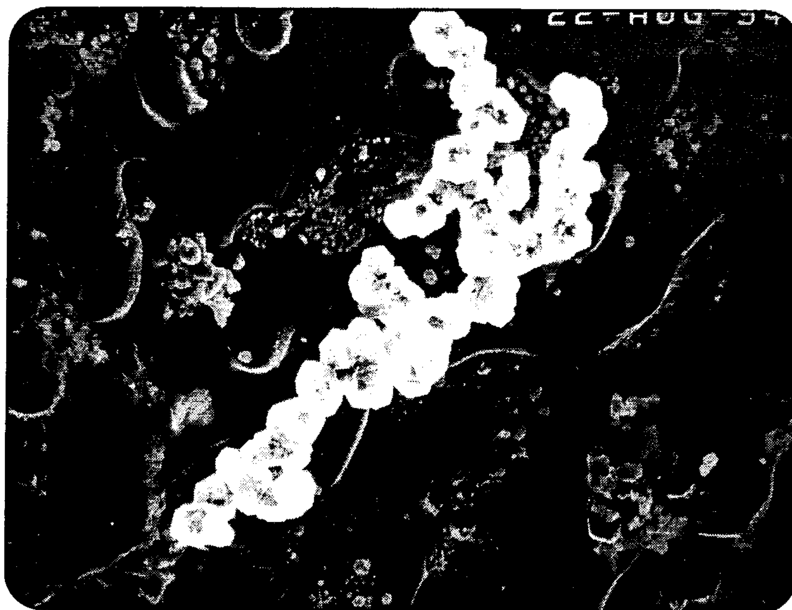

—— 10μm

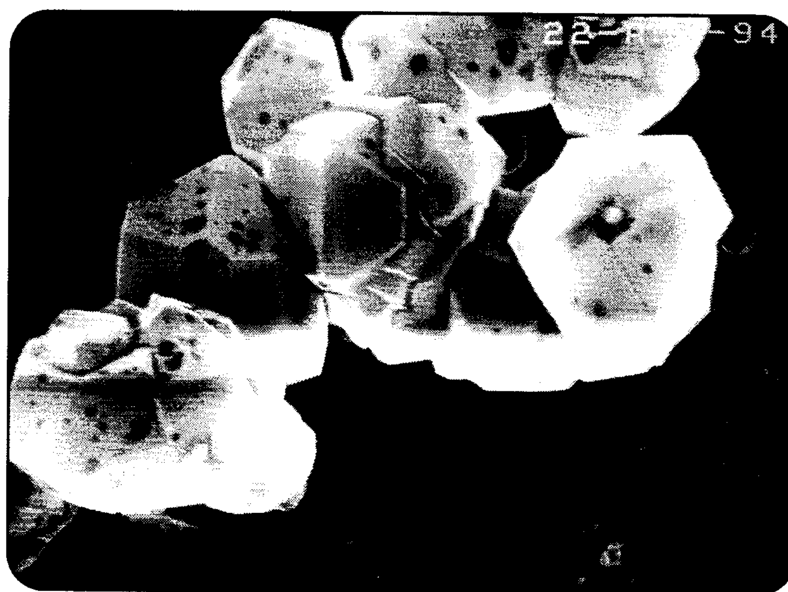

—— 3μm

Figure 10. Diamond particles on the surface of molten Ni-C ball.

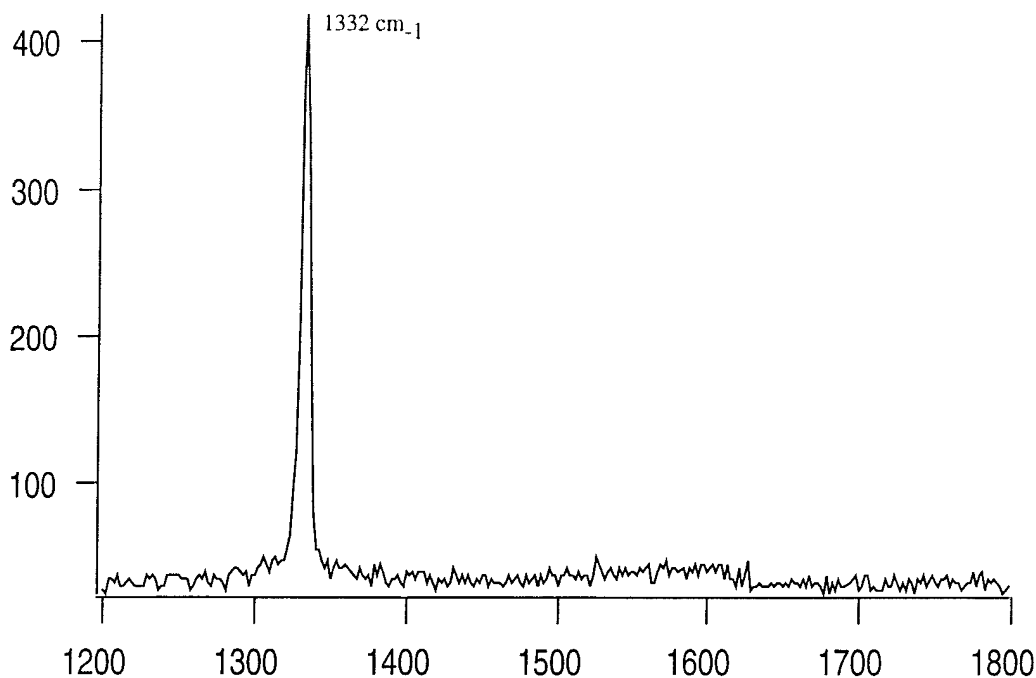

Figure 11. Micro-Raman spectrum on the diamond particles.

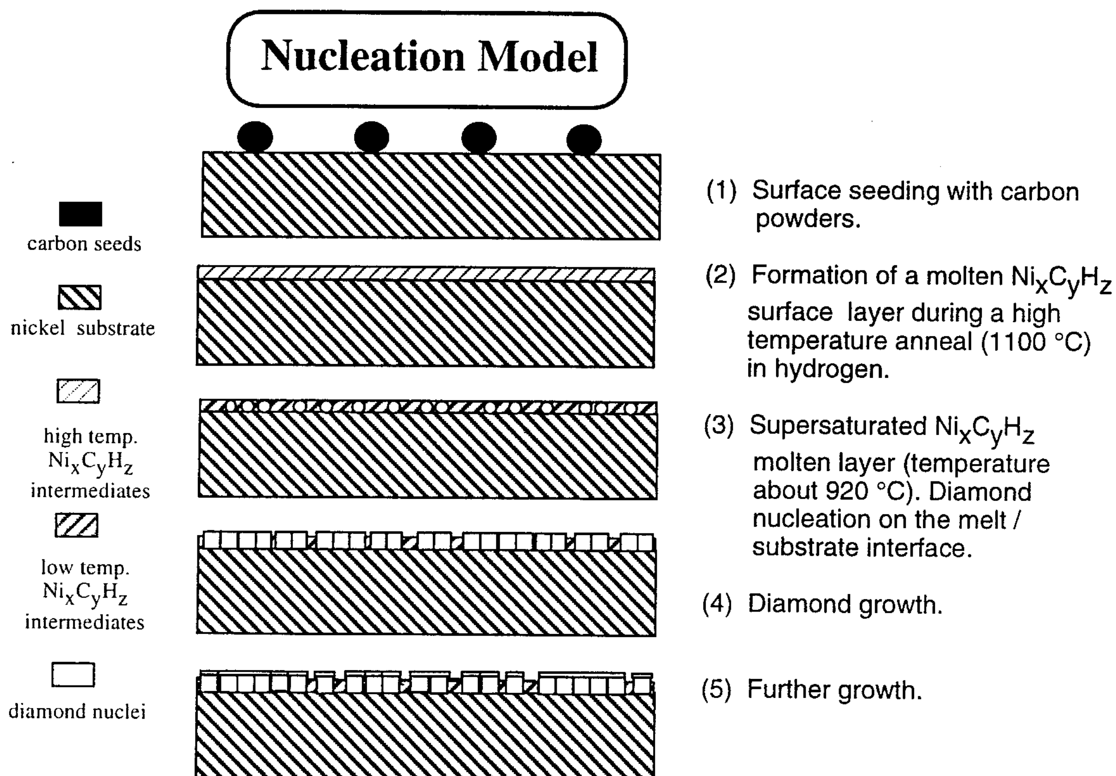

Figure 12. Nucleation model of the seeding and multi-step deposition process.

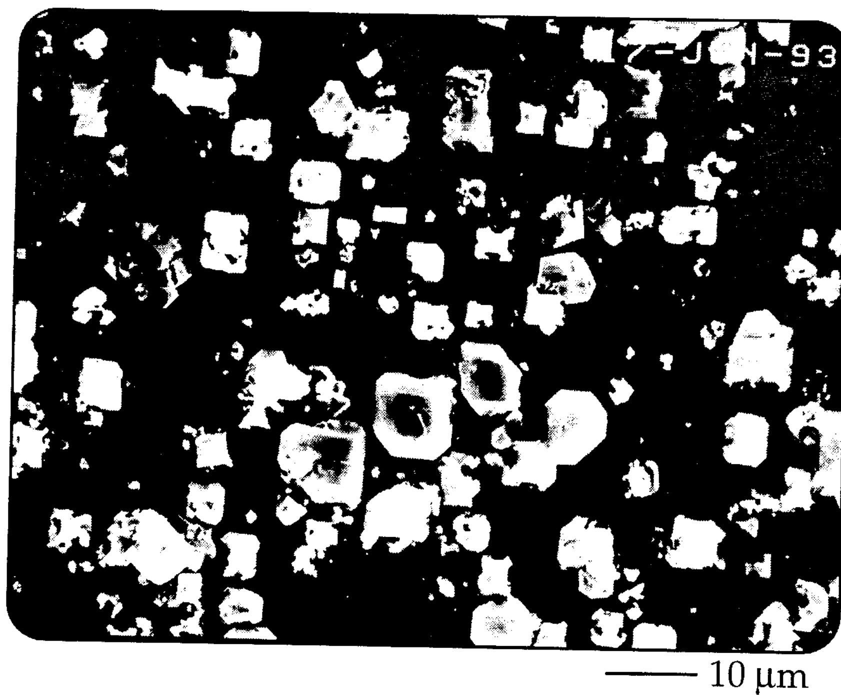

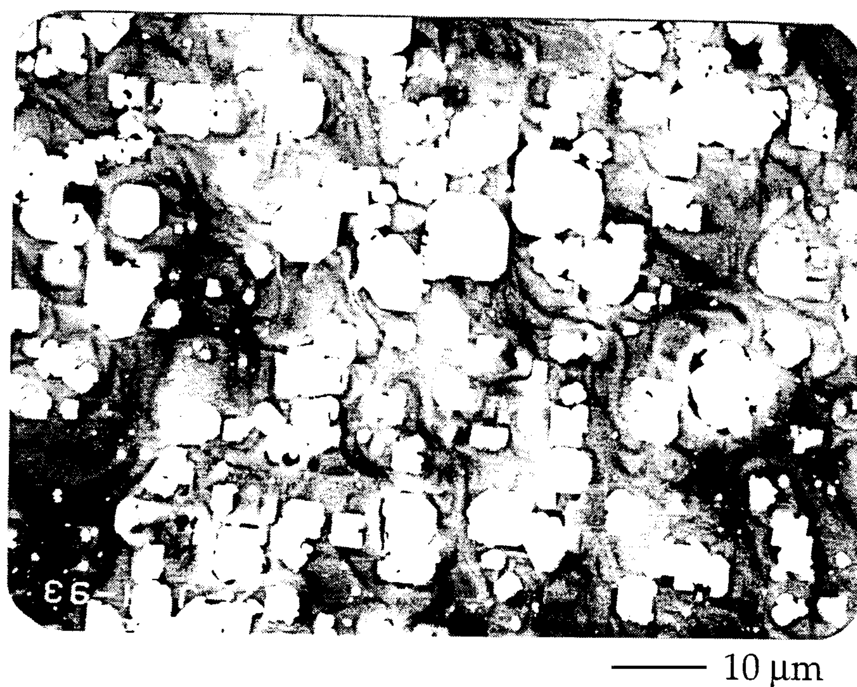

Figure 13. SEM micrographs of the (100) oriented diamond films on the Ni substrate with a different contrast in order to illustrate the evidence of surface melting and flow patterns.

The basic findings here are analogous to diamond formation using Ni by the HPHT process [12]. The free energy difference between non-diamond carbon and diamond at the high synthesis pressure and temperature results in graphite being more soluble than diamond in the same solvents. If the catalytic effects operate, diamond will crystallize from the solution. The nickel-carbon phase diagram at 57 kbars as worked out by Strong and Hanneman [13] shows that diamond crystallizes near the eutectic point from supersaturated C due to the solubility difference between diamond and graphite in Ni in the hypereutectic region. The temperature interval between the liquidus and the eutectic in this region is about 60°C. A similar mechanism is thought to exist in the multi-step process. However, the required energy is now supplied by atomic hydrogen instead of excessive pressures.

TEM Analysis of Oriented Growth Mechanism. The TEM and X-ray diffraction analysis shows the presence of the Ni_4C interlayer. The metastable Ni_4C carbide phase can be characterized as a NaCl-type structure with Ni occupying the fcc lattice positions of Na, and carbon occupies statistically some of the lattice positions of Cl, i.e. the octahedral interstitial sites of Ni lattice. Figure 14 depicts the (111) planes of Ni and carbon atoms in Ni_4C. The top layer is Ni and carbon atoms sit in the 3-fold interstitial position 1.04 Å beneath the surface Ni layer. In the figure the bold triangle shows an area where 6 nickel atoms lie on the surface and one carbon atom resides in the octahedral interstitial position. If a group of carbon atoms is now placed on top of each hollow position of this triangle, the effect of the interstitial C atom No. 1 on the No. 2 atom is different from that on the No. 3, 4, and 5 atoms. Under the influence of atomic hydrogen the interstitial carbon atom changes the electronic configuration of the Ni atoms. This difference affects the influence of interstitial carbon atoms on the alternate network and will tend to pucker the graphite plane network such that the sp^2 C is not stable. Therefore, an sp^3 C precursor could be formed. The same consideration can be applied to the case where the carbon atoms No. 3, 4, and 5 are on the tetrahedral position directly on top of the Ni atoms.

Yang and Whitten *et al.* [14] calculated the effects of subsurface Na, H and C on the bonding of carbon to nickel surfaces and conclude that tetrahedral CH_3 binds strongly to Ni(111) when an interstitial Na or H atom is present. The hydrogen calculation is in good agreement with the present experiments. Atomic H in the lattice appears to play a very important role in stabilizing the tetrahedral carbon bonding formation.

It is likely that the seeded carbon atoms dissolve into the surface Ni-C-H liquid as free atoms, and the intermediate Ni_4C phase will be formed under the influence of atomic hydrogen and catalytic properties of Ni. This Ni_4C structure will favor formation of a tetrahedral sp^3 C precursor and maintain the orientational relationship between diamond and Ni.

Liquid Phase Diamond Growth. The arguments of the previous two subsections apply to the liquid phase growth. The presence of atomic hydrogen facilitates the formation of a low temperature Ni-C-H eutectic. Upon cooling the carbon become supersaturated and precipitates

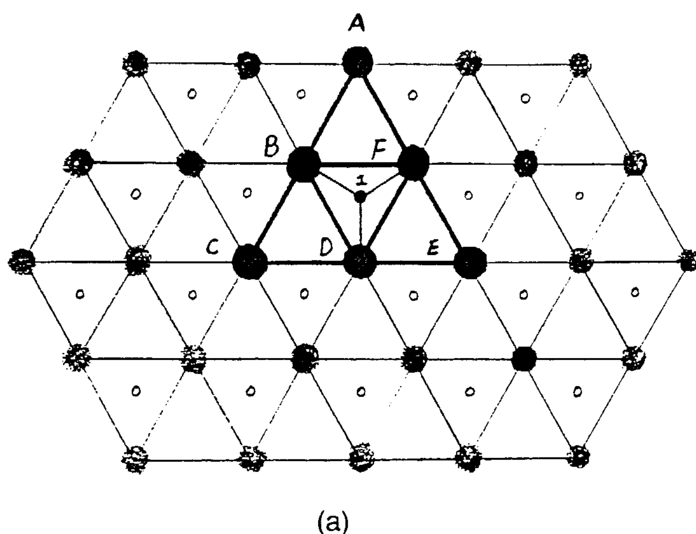

(a)

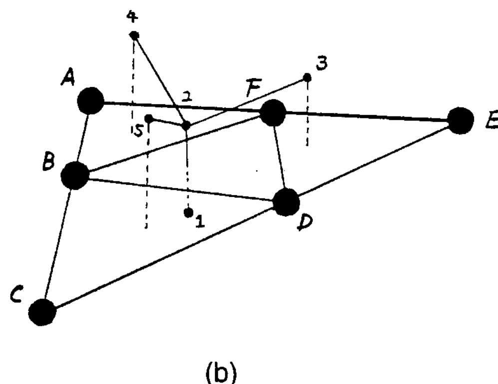

(b)

large shaded circle - Ni atoms
small light circle - C atoms

Figure 14. (a) Ni (111) planes with the carbon atoms in the interstitial sites 1.04Å beneath the Ni layer; (b) sp^3 C precursor originated from the Ni_4C structure.

on the surface as diamond. In fact, the success of the liquid phase experiments is further support for the existence of a molten surface phase. One would expect that a similar Ni_4C structure is formed prior to diamond precipitation, although that has not been investigated. One difference is that since the entire bulk is liquid, the orientation of the diamond particles is random.

E. Conclusions

Oriented diamond films have been achieved on both (100) and (111) single crystal Ni substrates using a multi-step method. *In-situ* laser reflectometry is used to monitor and control the process. Cross-sectional TEM and X-ray diffraction demonstrate the formation of a polycrystalline Ni_4C interlayer. A model is proposed to explain the nucleation mechanism, and structure arguments show why sp^3C precursors are stabilized on Ni_4C. The key to the process

involves a molten surface layer of Ni-C-H. The presence of atomic hydrogen dramatically reduces the melting temperature of this phase and facilitates the dissolution of seeded C into the Ni. Similarly, diamond growth has been demonstrated from liquid phase Ni-C in the presence of atomic hydrogen.

F. Future Research Plans and Goals

Oriented Diamond Growth. The focus of current work is directed at a better understanding of the surface molten phase. Specifically, the differential thermal analysis (DTA) is being used to determine the exact melting temperature as a function of composition. In addition, studies are planned using a microbalance to provide *in-situ* monitoring of mass changes. The reactor has been modified to allow for precise temperature control, and the process will be optimized with respect to the duration of the annealing stage (step 2), and the rate of cooling between step 2 and step 3.

In addition, future research work will concentrate on obtaining continuous, single crystal diamond films on Ni substrates. Because of the high solubility of C in Ni, a high growth rate is very important for getting highly oriented diamond facets to grow together (coalesce) after the nucleation stage by the seeding and multi-step process. We have demonstrated the growth of highly oriented <100> diamond films on Si substrates in a combustion growth system using pre-nucleated substrates prepared in a microwave bias enhanced growth system [15]. Similarly we plan to grow oriented films on samples that have been nucleated using the multi-step process. The growth rate of the combustion system is at least 10 μm/hour, which should favor growing out the oriented diamond nuclei to coalescence to form single crystal diamond films.

TEM Analysis of Oriented Growth Mechanism. The reactor has been modified to allow for rapid (>70° s^{-1}) quenching of samples. Quenched samples will be obtained from different stages of the multi-step process and subsequent SEM and TEM analysis will be performed to monitor microstructure evolution. In addition, chemical analysis is planned to ascertain the composition of the Ni-C-H phase.

Liquid Phase Diamond Growth. Having achieved diamond precipitation from the melt, the next step is controlling the precipitation and achieving it on a diamond or non-diamond seed. First of all, a top-seeded technique, will be used to grow diamond on a diamond seed or non-diamond seeds (such as Mo, W, and Al_2O_3). The critical parameters such as temperature control and viscosity of the solution need to be optimized. The seed will be chosen for lattice-match with diamond, chemical properties and physical shape, which are key factors for liquid phase growth. It is also very important to optimize the conditions to create enough atomic H to form the Ni-C-H intermediate state. By precise control of the degree of carbon supersaturation in the solution, the diamond can be precipitated from the Ni-C-H intermediate state and nucleated on the seed and then grown.

G. References

1. B. R. Stoner, D. M. Malta, A. J. Tessmer, J. Holmes, D. L. Dreifus, R. C. Glass, A. Sowers, and R. J. Nemanich, "Highly Oriented Diamond Films on Si: Growth, Characterization and Devices," in Proceedings of Diamond-Film Semiconductors, SPIE-The International Society for Optical Engineering, Los Angeles, California, (by the Society of Photo-Optical Instrumentation Engineers, (1994) p. 147.
2. P. C. Yang, W. Zhu, and J. T. Glass, Journal of Materials Research **8**, 1773 (1993).
3. C. Wild, R. Kohl, N. Herres, W. Müller-Sebert, and P. Koidl, Diamond and Related Materials **3**, 373 (1994).
4. H. P. Bovenkerk, F. P. Bundy, H. T. Hall, and H. M. Strong, Nature **184** (1959).
5. D. E. Ramaker, "CEELS as a Probe of the Carbide ite Transformation on Ni," in *Proceedings of New Diamond Science and Technology*, Washington, DC, Eds., J. T. G. Russell Messier, James E. Butler and Rustum Roy (Materials Research Society, 1991) p. 379.
6. D. N. Belton and S. J. Schmieg, Journal of Applied Physics **66**, 4223 (1989).
7. A. Badzian and T. Badzian, "Routes to diamond heteroepitaxy," in *Proceedings of Chemical Vapor Deposition of Refractory Metals and Ceramics II*, Boston, Massachusetts, Eds., T. M. Besmann, B. M. Gallois, and J. W. Warren (Materials Research Society, 1992) p. 339.
8. Y. Sato, H. Fujita, T. Ando, T. Tanaka, and M. Kamo, *Philosophical Transactions of the Royal Society of London* A **342**, 225 (1993).
9. T. J. Kistenmacher, Private Communication
10. R. Bernier, Ann. Chim. **6**, 104 (1951).
11. A. R. Badzian and A. Klokocki, Journal of Crystal Growth **52**, 843 (1981).
12. R. H. Wentorf, The Journal of Physical Chemistry **75**, 1833 (1971).
13. H. M. Strong, Acta Metallurgica **12**, 1411 (1964).
14. H. Yang, J. L. Whitten, and R. J. Markunas, Applied Surface Science **75** (1993) 12.
15. S. D. Trent, J. T. Glass, B. R. Stoner, and J. T. Prater, "Growth of Oriented Diamond Films via Ox-Acetylene Combustion," in *Proceedings of 5th Annual Diamond Technology Workshop*, Troy, MI, 1994) p. 65.

III. Properties of CeO_2 Films on Si(100) Substrates

A. Introduction

Thin films of CeO_2 deposited on silicon substrates may have the potential of providing MOS capacitor structures with a higher storage capacity compared to conventional SiO_2 films because of the higher relative dielectric constant (~ 26) of CeO_2 [1]. Epitaxial CeO_2 films deposited on Si(111) substrates by pulsed laser ablation of a CeO_2 target under UHV conditions at relatively high substrate temperatures in the range 550 to 750°C and annealed in different environments were previously investigated [2,3] and were shown to have improved electrical properties after annealing in oxygen at high temperature (900°C). This annealing was needed to reduce defects in the as-deposited films and retain their stoichiometry. This, however, resulted in the growth of an intermediate SiO_2 layer which increased the effective oxide thickness of MOS capacitors, and an optimization of the annealing time was generally needed [3]. Unlike other amorphous materials such as Ta_2O_5 [4], amorphous CeO_2 films have not been investigated for use in capacitor applications. These films can be deposited at lower temperatures which is expected to reduce oxygen deficiency and minimize the initial SiO_2 layer thickness of the films. Crystallization of these films on Si(100) substrates would be very interesting as a Silicon On Insulator (SOI) technology on Si(100) is preferred over a technology on Si(111) substrates for the lower density of surface states on (100) surfaces. This directly relates to a better performance of MOS devices fabricated on a (100) surface of an SOI substrate.

In this work, crystallization of CeO_2 films grown at low temperatures on Si(100) substrates was explored by rapid thermal annealing of a very thin film of CeO_2 grown at room temperature on an Si(100) substrate off-oriented by 4° in the <110> direction as enhanced partial crystallization of CeO_2 films grown by electron beam evaporation on such substrates was reported in the literature [5]. MOS capacitors were fabricated on the CeO_2 films deposited on silicon (100) substrates and characterized by C-V and I-V techniques.

B. Experimental Procedure

Five ohm-cm p-type Si(100) substrates off-oriented by 4° in the <110> direction were cleaned and degassed under UHV as previously described [2]. A preheat to 750°C for 10 minutes was carried out to evaporate contaminants from the silicon surface. The substrate temperature was then reduced to the growth temperature and pulsed laser ablation of a CeO_2 target (99.999% purity) was carried out under pressures lower than 5×10^{-8} Torr during the ablation. The growth temperatures were 20, 40 and 200°C.

Samples of films grown at 20°C of about 50 Å thickness were rapid thermally annealed in argon at 1000°C for 5 and 10 minutes and reloaded into the vacuum system to be examined by

RHEED. Samples of the films grown at 20 and 40°C were *ex situ* annealed in forming gas for 30 minutes at 500°C, and rapid thermally annealed in argon at 1000°C for 5 minutes. MOS capacitor structures were fabricated by evaporating aluminum dots onto the CeO_2 surface and the electrical properties of the films were investigated by C-V and I-V techniques. Films deposited at 200°C were *in situ* annealed at 750°C for 30 minutes. TEM revealed that partial coverage of the silicon surface took place at 200°C and no further work was done on these samples.

C. Results

Figure 1 shows the RHEED patterns observed of films of about 50 Å thickness grown at 20°C and rapid thermally annealed in argon at 1000°C for: (a) 5, and (b) 10 minutes. Figure 2 shows typical high frequency C-V characteristics obtained of as-grown, forming gas annealed ($N_2 + H_2$ for 30 min. at 500°C) and rapid thermally annealed (Ar for 5 min. at 1000°C) films of a thickness of about 300 Å. The breakdown voltages of capacitors fabricated on the as-grown films ranged from 2 to 13 volts with leakage currents of the order of 100 $\mu A/cm^2$ just before breakdown. For the forming gas annealed films, breakdown voltages between 8 and 14 volts were observed with almost the same leakage level before breakdown. For the rapid thermally annealed films lower breakdown voltages around 4 volts and higher leakage currents of about 500 $\mu A/cm^2$ were obtained.

D. Discussion

While the RHEED pattern in Fig.(a) indicates that the films were amorphous even after the RTA for 5 minutes, fading streaks appear in the pattern of Fig.(b) which can indicate a partial crystallization at the films surface after 10 minutes annealing. However, the patterns observed in some spots of the 10 minutes annealed films had bright rings which suggests that another technique is needed to achieve single-crystallization of the films on top of the Si(100) template.

As can be seen from Fig. 2(a), large accumulation capacitances were obtained from as-deposited amorphous films of CeO_2. The value of 2500 pF corresponds to an effective SiO_2 thickness of 8.5 nm of the MOS capacitors. The leakage level of these samples was, however, excessively high resulting in inclined C-V curves in accumulation and deep depletion under positive voltages as inversion charges had probably leaked through the films. Their breakdown voltages varied largely depending probably on the presence of local defects in the films. Forming gas annealing appears to improve the leakage characteristics. Leakage current effects on the C-V curves were less pronounced as can be seen from Fig. 2(b). The films had breakdown voltages which are larger and less scattered in value than those of as-grown films. The capacitance obtained in accumulation was slightly less due probably to the formation of a thin layer of SiO_2 by oxygen to the silicon surface. The annealing temperature which is 500°C

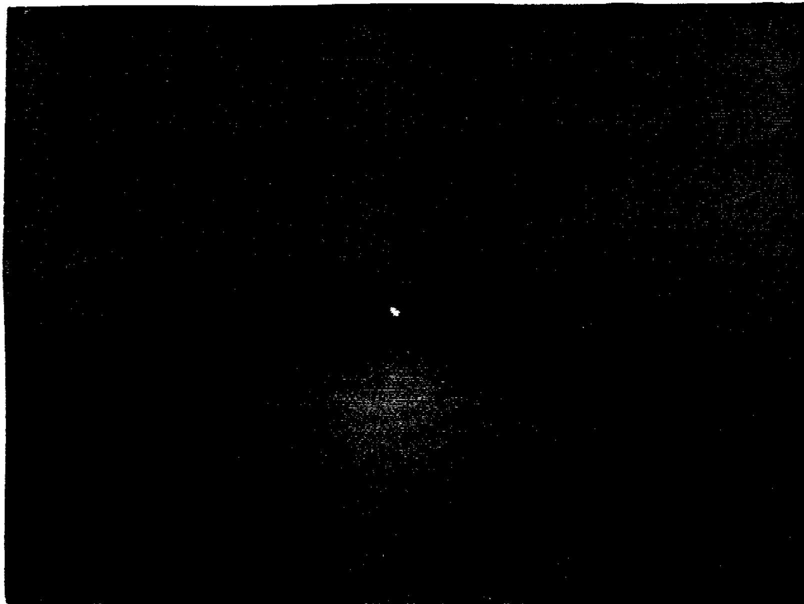

Figure 1(a). RHEED pattern observed of CeO_2 films of about 50 Å deposited at 20°C on Si(100) and rapid thermally annealed in argon at 1000°C for 5 minutes.

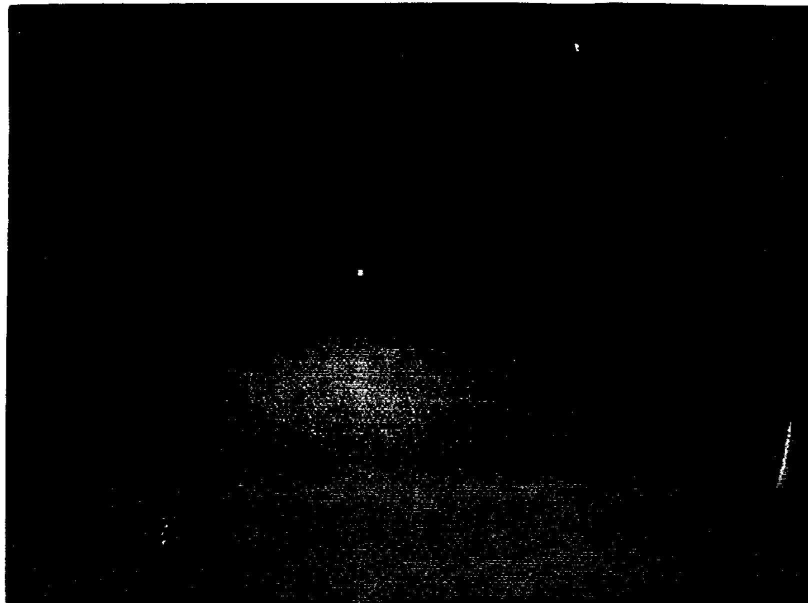

Figure 1(b). RHEED pattern observed of CeO_2 films of about 50 Å deposited at 20°C on Si(100) and rapid thermally annealed in argon at 1000°C for 10 minutes.

is lower than values where the stoichiometry of the films would be affected by a low partial pressure of oxygen in the annealing ambient [6,7]. However, still deep depletion of the silicon surface under positive biases was observed. Films exposed to rapid thermal annealing in argon at 1000°C for 5 minutes had degraded C-V characteristics as seen from Fig. 2(c). They did not reach a maximum capacitance in accumulation up to -10 volts as accumulation charges could have been leaking through the films. The leakage levels of these films were higher than those

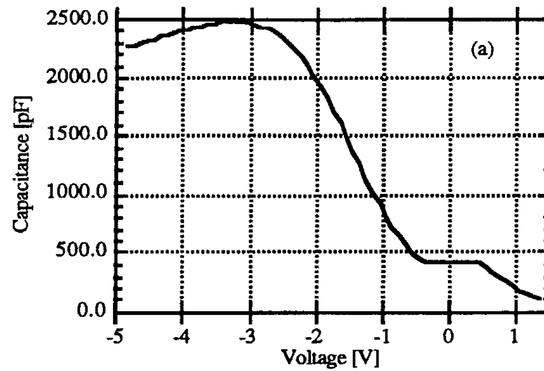

Fig. 2(a). High frequency C-V curves of MOS capacitors with 35 mils diameter fabricated on as-grown CeO_2 films with a thickness of about 300 Å deposited on Si(100) at 40°C, at a frequency of 100 KHz.

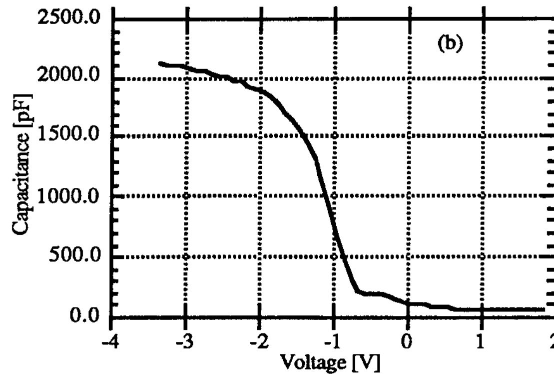

Fig. 2(b). High frequency C-V curves of MOS capacitors with 35 mils diameter fabricated on CeO_2 films with a thickness of about 300 Å deposited on Si(100) at 40°C and annealed in forming gas ($N_2 + H_2$) for 30 min at 500°C, at frequency of 1 MHz.

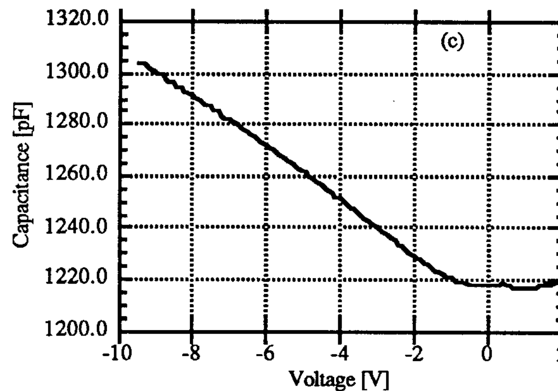

Fig. 2(c). High frequency C-V curves of MOS capacitors with 35 mils diameter fabricated on CeO_2 films with a thickness of about 300 Å deposited on Si(100) at 40°C and rapid thermally annealed in Ar for 5 min. at 1000°C, at a frequency of 100 KHz.

of as-deposited films and their breakdown voltages were lower than those of films annealed in forming gas at 500°C. This can be a result of partial crystallization of the films into polycrystalline CeO_2 or an increase in oxygen deficiency of the films with annealing.

E. Conclusions

Films of CeO_2 were deposited at lower temperatures on Si(100) substrates. Crystallization of very thin CeO_2 films deposited on 4° off-oriented Si(100) by rapid thermal annealing in an argon environment at 1000°C for 5 and 10 minutes was investigated. The RHEED patterns observed indicated partial crystallization at the films surface.

Samples of the deposited films were annealed in forming gas at 500°C for 30 minutes and rapid thermally annealed in argon at 100°C for 5 minutes. The as-grown and annealed samples were characterized by C-V and I-V techniques to explore their potential for use in MOS memory devices. Relatively high accumulation capacitance and high leakage currents were observed of as-grown films. Improved leakage and breakdown characteristics were obtained with forming gas annealing while the rapid thermal annealing resulted in enhanced leakage through the films.

E. Future Research Plans and Goals

Crystallization of CeO_2 films on Si(100) surfaces for a SOI technology on Si(100) substrates is very interesting and will be further investigated. Ways to reduce the leakage currents of as-deposited amorphous CeO_2 films on silicon substrates are also to be investigated. Characterization of MOS capacitors of epitaxial CeO_2 films on Si(111) substrates with optimized oxygen annealing times is now in progress and will soon be reported.

F. References

1. T. Inoue, M. Osonoe, H. Tohda, M. Hiramatsu, Y. Yamamoto, A. Yamanaka and T. Nakayama, J. Appl. Phys. **69**, 8313 (1991).
2. T. Chikyow, L. Tye, N. El-Masry and S. Bedair, Appl. Phys. Lett. **65**, 1030 (1994).
3. A. H. Morshed, M. Tomita, P. McLarty, N. Parihk, N. El-Masry and S. Bedair, Materials Research Society Meeting Fall 1994, Boston, MA.
4. S. O. Kim and H. J. Kim, Thin Solid Films **253**, 435 (1994).
5. T. Inoue, H. Kudo, T. Fukusho, T. Ishihara, T. Ohsuna, Jpn. J. Appl. Phys. **33**, L139 (1994).
6. P. Kofstad, *Non-Stoichiometry, Diffusion and Electrical Conductivity in Binary Metal Oxides*, Wiley Interscience, 1972, p.277.
7. H. Tuller and A. Nowick, J. Electrochem. Soc. **126**, 209 (1979).

IV. Distribution List

Mr. Max Yoder Office of Naval Research Electronics Division, Code 312 Ballston Tower One 800 N. Quincy Street Arlington, VA 22217-5660	3
Administrative Contracting Officer Office of Naval Research Regional Office Atlanta 101 Marietta Tower, Suite 2805 101 Marietta Street Atlanta, GA 30323-0008	1
Director, Naval Research Laboratory ATTN: Code 2627 Washington, DC 20375	1
Defense Technical Information Center Bldg. 5, Cameron Station Alexandria, VA 22314	2